This article was downloaded by: [Renmin University of China]
On: 13 October 2013, At: 10:43
Publisher: Taylor & Francis
Informa Ltd Registered in England and Wales Registered Number: 1072954 Registered office: Mortimer House, 37-41 Mortimer Street, London W1T 3JH, UK

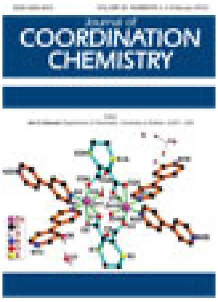

Journal of Coordination Chemistry
Publication details, including instructions for authors and subscription information:
http://www.tandfonline.com/loi/gcoo20

Luminescent nine-coordinate lanthanide complexes derived from fluorinated β-diketone and 2,4,6-tris(2-pyridyl)-1,3,5-triazine

Rashid Ilmi [a] & K. Iftikhar [a]

[a] Department of Chemistry, Jamia Millia Islamia, New Delhi 110 025, India

Published online: 24 Jan 2012.

To cite this article: Rashid Ilmi & K. Iftikhar (2012) Luminescent nine-coordinate lanthanide complexes derived from fluorinated β-diketone and 2,4,6-tris(2-pyridyl)-1,3,5-triazine, Journal of Coordination Chemistry, 65:3, 403-419, DOI: 10.1080/00958972.2011.649737

To link to this article: http://dx.doi.org/10.1080/00958972.2011.649737

PLEASE SCROLL DOWN FOR ARTICLE

Taylor & Francis makes every effort to ensure the accuracy of all the information (the "Content") contained in the publications on our platform. However, Taylor & Francis, our agents, and our licensors make no representations or warranties whatsoever as to the accuracy, completeness, or suitability for any purpose of the Content. Any opinions and views expressed in this publication are the opinions and views of the authors, and are not the views of or endorsed by Taylor & Francis. The accuracy of the Content should not be relied upon and should be independently verified with primary sources of information. Taylor and Francis shall not be liable for any losses, actions, claims, proceedings, demands, costs, expenses, damages, and other liabilities whatsoever or howsoever caused arising directly or indirectly in connection with, in relation to or arising out of the use of the Content.

This article may be used for research, teaching, and private study purposes. Any substantial or systematic reproduction, redistribution, reselling, loan, sub-licensing, systematic supply, or distribution in any form to anyone is expressly forbidden. Terms & Conditions of access and use can be found at http://www.tandfonline.com/page/terms-and-conditions

Journal of Coordination Chemistry
Vol. 65, No. 3, 10 February 2012, 403–419

Luminescent nine-coordinate lanthanide complexes derived from fluorinated *β*-diketone and 2,4,6-*tris*(2-pyridyl)-1,3,5-triazine

RASHID ILMI and K. IFTIKHAR*

Department of Chemistry, Jamia Millia Islamia, New Delhi 110 025, India

(*Received 12 September 2011; in final form 22 November 2011*)

The synthesis, photoluminescence, 4f–4f absorptions, and NMR studies of nine-coordinate lanthanide(III) complexes, [Ln(tfaa)$_3$(tptz)] (Ln = La, Nd, Sm, and Eu; tfaa is the anion of 1,1,1-trifluoro-2,4-pantanedione; and tptz = 2,4,6-*tris*(2-pyridyl)-1,3,5-triazine), are reported. These complexes are synthesized in a single pot by *in situ* method and thoroughly characterized. The *β*-diketone and tptz chemical shifts, in the cases of paramagnetic complexes, are in the opposite directions. The lanthanide-induced shifts are dipolar in nature. The luminescence and 4f–4f absorptions are analyzed and discussed. The samarium and europium complexes emit strong pink and red luminescences due to $^4G_{5/2} \rightarrow {}^6H_j$ (j = 5/2, 7/2, 9/2) and $^5D_0 \rightarrow {}^7F_j$ (j = 0–4) transitions, respectively. The $^4G_{5/2} \rightarrow {}^6H_{7/2}$ (607 nm) emission transition of Sm(III) has no Stark components and indicates a higher local symmetry around Sm(III). The very strong hypersensitive $^5D_0 \rightarrow {}^7F_2$ transition of Eu reflects a highly polarizable chemical environment around Eu(III). The absorption spectra of the neodymium complex are investigated and analyzed.

Keywords: Lanthanide; 2,4,6-Tris(2-pyridyl)-1,3,5-triazine; 1,1,1-Trifluoro-2,4-pentanedione; 4f–4f Absorption; Hypersensitivity; Luminescence

1. Introduction

Stable luminescent complexes of trivalent lanthanides have important applications such as light-emitting sensors for hetero- and homogeneous fluoroimmunoassays [1], light emitting diodes and display devices [2], luminescent probes [3], lasers [4], and biological imaging applications [5, 6]. Trivalent lanthanides are an interesting alternative for two main reasons. First, electrons of the filled 5s and 5p orbitals shield the 4f electrons against interaction with the surroundings. As a consequence, the intraconfigurational 4f–4f emission transitions of the lanthanide ions are little affected by the environment and give atom-like emission spectra with very sharp bands (a few nm). Second, they present the unique advantage of having ion-specific emission. Depending on the lanthanide ion, emission colors from blue to the near-infrared (IR) can be obtained.

The *β*-diketones have been widely used in lanthanide chemistry for several reasons, (i) they afford thermodynamically stable volatile photo-luminescent compounds [7, 8], (ii) possess high absorption coefficients in the UV range, and (iii) their excited states

---

*Corresponding author. Email: kiftikhar@jmi.ac.in

Journal of Coordination Chemistry
ISSN 0095-8972 print/ISSN 1029-0389 online
http://dx.doi.org/10.1080/00958972.2011.649737

possess suitable energy levels for providing efficient energy transfer (antenna effect) to the visible and near-IR emitting lanthanide ions [9–11]. Because of being coordinatively unsaturated, lanthanide *tris*(β-diketonates) easily bind more ligands such as NN diimine [12–15] or NN bisdiimine [16–18] to achieve higher coordination numbers (8–10) [12–17]. We have recently investigated the antenna effect of bidentate and tetradentate neutral heterocyclic diimines coordinated to the lanthanide *tris*(β-diketonates) and have reported their absorption and luminescent properties [15–20]. Ligands are important in modifying the luminescent properties of the lanthanide complexes. One neutral ligand is the tridentate 2,4,6-tri(2-pyridyl)-1,3,5-triazine (tptz), a bulky aromatic compound featuring three 2-pyridyl rings fixed on a central 1,3,5-triazine platform with large π-systems for stabilization and strong coordinating ability [21]. There are a few structurally characterized lanthanide complexes in which tptz is a tridentate ligand [22–24]. Zheng and co-workers in an attempt to synthesize [Eu(hfaa)$_3$(tptz)], where hfaa is the anion of 1,1,1,5,5,5-hexaflouro-2,4-pentanedione, adopted two routes [24b]. The first route was a one-pot *in situ* synthesis that did not give the desired product. However, the second route which was a two-step reaction (isolation first of the chelate and then its reaction with tptz) did give the desired product in 67% yield. We have used an alternate, one-pot *in situ*, method to synthesize [Ln(tfaa)$_3$tptz] complexes using ammonium hydroxide (instead of potassium butoxide [24b]) and have isolated the complexes in very good yield (>80%). Here we report a modified route for the synthesis of [Ln(tfaa)$_3$tptz] (Ln = La, Nd, Sm, and Tb) and solution properties (optical absorption, hypersensitivity, photoluminescence, and nuclear magnetic resonance (NMR)) of these new highly luminescent nine-coordinate complexes.

2. Experimental

2.1. *Materials*

Commercially available chemicals were used without purification, Ln$_2$O$_3$ (Ln = La, Nd, Sm, and Eu 99.99%) from Aldrich. These oxides were converted to their corresponding chlorides. 2,4,6-Tri(2-pyridyl)-1,3,5-triazine (tptz) (Aldrich) and 1,1,1-trifluoro-2,4-pentanedione (Htfaa) (Lancaster, England) were used as received. The solvents used in this study were of AR/spectroscopic grade.

2.2. *Methods*

Elemental analyses were performed at Delhi University, New Delhi, India. NMR spectra were recorded on a BRUKER AVANCE II 400 NMR spectrometer. IR spectra were recorded on a Perkin-Elmer spectrum RX I FT-IR spectrophotometer as KBr discs from 4000 to 400 cm^{-1}. The melting points of the complexes were recorded by conventional capillary methods as well as on a DSC instrument in aluminum pans at a heating rate of 10°C min^{-1}. Thermal studies were carried out under dinitrogen on Exstar 6000 TGA/DTA and DSC 6220 instruments from SIINT, Japan. The electrospray ionization mass spectra of the complexes in positive ion mode were recorded on a Waters Micromass Q-T mass spectrometer. The electronic spectra of [Nd(tfaa)$_3$(tptz)] and [Nd(tfaa)$_3$H$_2$O] were recorded on a Perkin-Elmer Lambda-40 spectrophotometer, with the samples contained in 1 cm^3 stoppered quartz cells of 1 cm path length, from 200 to 1100 nm, at concentrations between 5×10^{-3} and 6×10^{-3} mol L^{-1}. Steady state room temperature emission/excitation spectra were recorded on a Fluorolog 3–22 Spectrofluorimeter from Horiba–Jobin Vyon, using a 450 W Xenon lamp as the excitation source and equipped with a R928P Hamamatsu photomultiplier tube as detector. The samples were contained in a 10 mm Quartz Fluorometer Cell with stopper from Starna Cells, Inc.

2.3. *Synthesis of [Ln(tfaa)$_3$H$_2$O]*

[Ln(tfaa)$_3$H$_2$O] (Ln = Nd, Sm, and Eu) were synthesized by a simple method. The synthesis of [Nd(tfaa)$_3$H$_2$O] is given here as representative.

2.3.1. [Nd(tfaa)$_3$H$_2$O]. Htfaa (0.80 mL, 6.48 mmol) was transferred in a 25 mL beaker containing 10 mL distilled water. Dilute ammonium hydroxide solution was added to this mixture. Initial addition of NH_4OH solution results in the formation of two layers. Controlled addition of NH_4OH solution was continued until a homogeneous solution appeared. A solution of $NdCl_3 \cdot 6H_2O$ (0.77 g, 2.16 mmol) in water was then added to the ammonium trifluoroacetylacetone solution with constant stirring. The reaction mixture was stirred at room temperature for ~7 h. The neodymium *tris*(trifluoroacetylacetonate) was precipitated. The complex was filtered off, washed with water, and dried in air. The pure product was obtained by repeated crystallization from chloroform several times. It was thoroughly characterized before use.

2.4. *Synthesis of [Ln(tfaa)$_3$(tptz)]*

All the complexes were synthesized by a similar *in situ* method (scheme 1). The synthesis of [La(tfaa)$_3$tptz] is given here as representative.

2.4.1. [La(tfaa)$_3$(tptz)]. A solution of Htfaa (0.50 g, 3.2 mmol) in ethanol (5 mL) was added to 0.24 mL (0.054 g, 3.2 mmol) 25% ammonia solution. This mixture in a 50 mL beaker was covered until all the ammonia vapors dissolved. To this mixture, 5 mL ethanol solution of tptz (0.3378 g, 1.07 mmol) and 5 mL ethanol solution of $LaCl_3 \cdot 6H_2O$ (0.4016 g, 1.07 mmol) was added. The reaction mixture was stirred at room temperature for 5 h. A white precipitate appeared during stirring which was filtered off repeatedly. The filtrate was covered and left for slow solvent evaporation at room temperature. A colorless product appeared after 3 days, which was filtered off and washed with $CHCl_3$ several times. The product thus obtained was recrystallized twice from ethanol to get pure compound and dried under *vacuum* over P_4O_{10}. Color (white); yield (82%); Elemental analysis (Found (%): C, 43.65; H, 2.73; N, 9.29. Calcd $C_{33}H_{24}O_6F_9N_6La$ (%): C, 43.53; H, 2.65; N, 9.23). m.p. 216°C. A similar procedure was employed to synthesize the other lanthanide complexes.

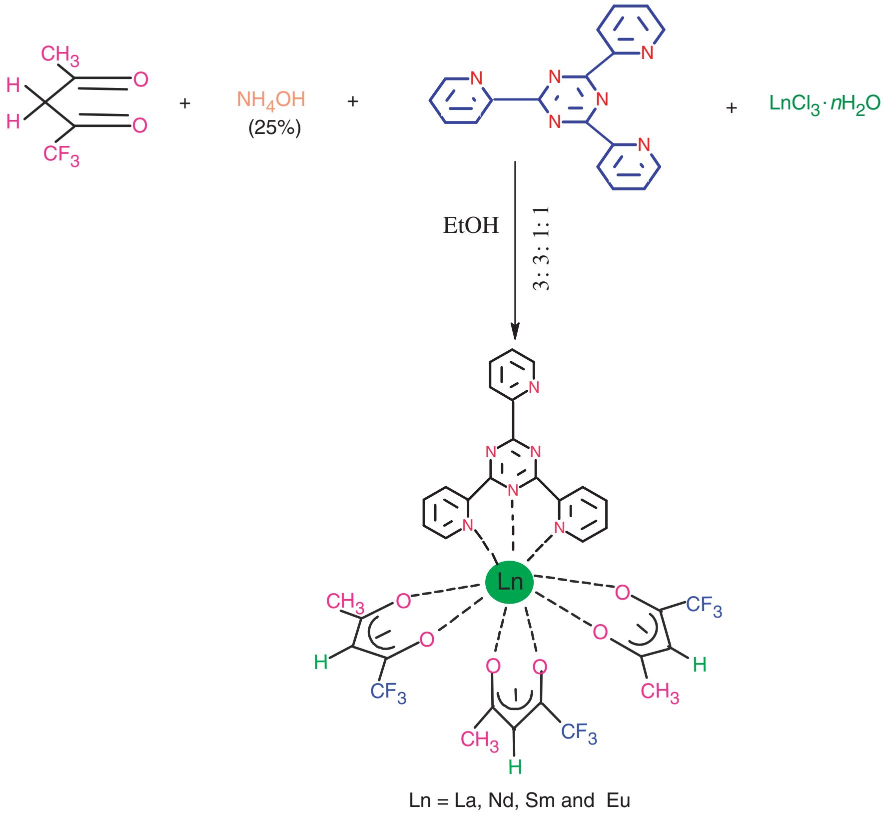

Scheme 1. Reaction pathway.

2.4.2. [Nd(tfaa)$_3$(tptz)]. Color (lilac); yield (83%); Elemental analysis (Found (%): C, 43.39; H, 2.75; N, 9.26. Calcd $C_{33}H_{24}O_6F_9N_6Nd$ (%): C, 43.27; H, 2.64; N, 9.17). m.p. 212°C.

2.4.3. [Sm(tfaa)$_3$(tptz)]. Color (dirty white); yield (81%); Elemental analysis (Found (%): C, 43.11; H, 2.69; N, 9.18. Calcd $C_{33}H_{24}O_6F_9N_6Sm$ (%): C, 42.99; H, 2.62; N, 9.11). m.p. 205°C.

2.4.4. [Eu(tfaa)$_3$(tptz)]. Color (pale yellow); yield (83%); Elemental analysis (Found (%): C, 43.01; H, 2.67; N, 9.21. Calcd $C_{33}H_{15}O_6F_9N_6Eu$ (%): C, 42.91; H, 2.61; N, 9.09). m.p. 206°C.

3. Results and discussion

Nine-coordinate complexes of La(III), Nd(III), Sm(III), and Eu(III), [Ln(tfaa)$_3$tptz], were synthesized by a modified one-pot *in situ* method in high yield in which trifluoroacetylacetone, ammonium hydroxide (25% ammonia), tptz and $LnCl_3 \cdot nH_2O$

were mixed in a single pot in a 3 : 3 : 1 : 1 molar ratio in ethanol at room temperature. There are three advantages of the method we employed: (i) the reaction is carried out in air, (ii) the reaction temperature was ambient, and (iii) it gives the product in very high yield (> 80%). These complexes were characterized by melting point, elemental analysis, IR, TGA/DTA, ESI-MS, and NMR studies. The stoichiometry is based on the assumption that tptz is a tridentate ligand and nine-coordinate trifluoroacetylacetone tptz complexes would be formed. For all the lanthanides used in this study, this assumption was found to be correct (scheme 1), as clearly shown by the elemental analysis. Air and moisture stable nine-coordinate complexes were isolated in more than 80% yield. These complexes are readily soluble in acetone, chloroform, and dichloromethane and are soluble in alcohols upon heating. Although tptz is a flexible ligand, the thermal stability of its complexes is at par with those of [Ln(tfaa)$_3$phen] [25]. The ES$^+$ MS spectra of the lanthanum and samarium complexes (figures S1 and S2) show molecular ion peaks at a m/z ratio of 911 and 922 due to the parent ion $[\mathrm{La(tfaa)_3(tptz)} + \mathrm{H}^+]^+$ and $[\mathrm{Sm(tfaa)_3(tptz)} + \mathrm{H}^+]^+$, respectively. No peak corresponding to $m/z = 598$ for $[\mathrm{Ln(tfaa)_3} + \mathrm{H}]^+$ is observed. These diverse ionic species can be accounted for in terms of fragmentation, ligand exchange, and clustering reactions. Such reactions are also observed in the ESI-mass spectra of lanthanide β-diketone complexes [26].

The IR spectrum of tptz displays peaks at 1369 and 994 cm^{-1}, which are assigned to the breathing vibration of the central ring and the bending vibration of the pyridyl ring, respectively. The position of these bands (figure S3) are shifted by 11–14 and 14–17 cm^{-1}, respectively, in the complexes, indicating that the central ring nitrogen and pyridyl nitrogen are coordinated to lanthanide [27].

3.1. *Thermal analysis*

Since thermal stability is important in the fabrication of electro-luminescent layers, the complexes were subjected to thermal analysis. Unlike other fluorinated β-diketone complexes of lanthanides, for instance Hfaa [15] and Hfod [16] (where fod is the anion of 6,6,7,7,8,8,8-heptafluoro-2,2-dimethyl-3,5-octanedione), the tfaa complexes are not volatile and decompose after melting. The thermograms of the complexes do not exhibit any weight loss up to 240°C, which clearly indicates that the complexes are anhydrous. The thermograms of the Sm and Eu complexes (figure S4) display one endothermic peak at 205°C and 206°C, respectively, representing melting of the complexes while decomposition occurs after melting. The observed wt. losses of 49.5% and 48.6% represent the removal of 3 tfaa units (theoretically Calcd wt. loss for three tfaa is 50% for Sm and Eu). The expulsion of tptz begins after the removal of tfaa units. The observed wt. loss of 28.6–30% between 350°C and 550°C corresponds well with the loss of tptz (Calcd wt. loss for tptz is 32%). This reflects that tptz is more strongly attached than tfaa.

3.2. *NMR spectra*

3.2.1. Diamagnetic complex. NMR spectra of complexes of La, Nd, Sm, and Eu, recorded in CDCl$_3$, are first-order spectra and consistent with the presence of coordinated β-diketones and tptz. Assignment of NMR signals is based on comparison of the spectra of the individual complex with the spectrum of free tptz and relative intensities and spin–spin splittings. The chemical shifts (δ) and paramagnetic shifts ($\Delta\delta$) are given in table 1. The NMR spectrum of the lanthanum complex (figure S5) displays nine signals, two due to the β-diketone (methine and methyl protons) and seven due to tptz. Resonances appearing at 5.52 and 1.84 ppm (δ), which integrate for three and nine protons, have been assigned to methine (–CH) and methyl (–CH_3) groups of tfaa, respectively. The rest of the signals appearing at 9.00 (d), 8.86 (d), 8.82 (d), 8.05 (t), 8.00 (s), 7.63 (t), 7.59 (s) ppm (δ) have been assigned to H6,6 and H6′; H3,3, H3′; H4,4, H4′; H5.5, and H5′ of coordinated tptz, respectively. A significant downfield shift of the signals of all protons of metal-bound pyridyl rings of tptz is observed as compared to their positions in free tptz. The intensity ratio between the methine protons and tptz protons is 3 : 12, indicating that only one tptz unit has coordinated to the metal.

3.2.2. Paramagnetic complex.

Structural information may be gained from the analysis of NMR spectra of the paramagnetic complexes (Nd, Sm, and Eu). The tptz protons are shifted to higher fields (in the cases of Nd and Sm) and lower fields (in the case of Eu) as compared to the diamagnetic analogue, indicating delocalization of unpaired electron density into the aromatic ligand. The paramagnetic shift is produced by an interaction between the nuclear magnetic moment of the diamagnetic nuclei and the magnetic field produced by the unpaired f-electrons of the lanthanides. This interaction occurs in a through-space dipole–dipole manner or by delocalization of f-electron density towards the resonating nucleus through the bonds. As a result of through-space (dipolar) or through-bond (contact) interactions between the electronic spin in the paramagnetic Ln(III) ion and the nuclear spins of the diamagnetic ligand nuclei, the resonance of a given proton is markedly shifted from the position observed in a diamagnetic environment. However, in lanthanides the radial extension of the 4f-orbitals is exceedingly small since electrons in these orbitals are shielded from the ligand by 5s and 5p electrons. Consequently, contact interactions are diminished and the induced chemical shifts arise predominantly from the dipolar mechanism which can provide information relating geometrical configuration of the ligands around a metal ion in solution.

Table 1. Chemical shifts (δ) and paramagnetic shifts ($\Delta\delta$) of the complexes.[a]

Compound		$H_{6,6}$	$H_{3,3}$	$H_{4,4}$	$H_{5,5}$	$H_{6'}$	$H_{3'}$	$H_{4'}$	$H_{5'}$	CH	CH_3
tptz		8.99	8.91	8.01	7.58	–	–	–	–	–	–
[La(tfaa)$_3$(tptz)]	1	9.00(d)	8.86(d)	8.05(t)	7.63(t)	9.00(d)	8.82(d)	8.00(s)	7.59(s)	5.52	1.84
[Nd(tfaa)$_3$(tptz)]	2	−8.94(s)	3.75(d)	5.94(t)	6.65(d)	2.19(s)	8.42(s)	7.48(t)	7.57(d)	10.6	2.99
		(−17.94)	(−5.11)	(−2.11)	(−0.98)	(−6.81)	(−0.4)	(−0.52)	(−0.02)	(5.11)	(1.15)
[Sm(tfaa)$_3$(tptz)]	3	3.02(s)	8.34(d)	6.28(t)	7.33(t)	8.96(d)	8.73(d)	7.99(t)	7.59(t)	6.97	2.28
		(−5.98)	(−0.52)	(−1.77)	(−0.3)	(−0.04)	(−0.09)	(−0.01)	(0.0)	(1.45)	(0.44)
[Eu(tfaa)$_3$(tptz)]	4	31.5(s)	12.48(d)	10.60(t)	10.53(d)	9.70(d)	9.40(d)	8.41(t)	7.87(t)	1.25	0.65
		(22.50)	(3.62)	(2.55)	(2.99)	(0.70)	(0.58)	(0.41)	(0.28)	(−3.8)	(−1.19)

s – singlet; d – doublet; t – triplet.

[a] The paramagnetic shift ($\Delta\delta$) given in parentheses is the difference between the chemical shift of the nucleus in the paramagnetic complex and corresponding shift in the diamagnetic complex.

For the paramagnetic complexes studied, the changes produced in the chemical shifts of tptz resonances are approximately equal, although the magnitude and direction of such changes are a function of the central metal which can be related to the magnetic anisotropy of the lanthanide(III). Among the three lanthanide complexes (Nd, Sm, and Eu), the largest upfield shifts are noted for the neodymium complex and becoming relatively small for samarium and changing sign at europium which causes downfield shifts; induced shifts rapidly decrease with increasing distance of the nucleus from the lanthanide ion (figures 1 and 2). The H_{66} signal of tptz for the neodymium complex is substantially upfield shifted compared to its position in the diamagnetic lanthanum complex and appears as a sharp signal at −8.94 ppm (δ). The sharp, strong signal at 10.63 ppm (δ) has been assigned to the methine proton of tfaa which is significantly downfield shifted. Thus, the Nd complex covers a chemical shift range of 19.60 ppm (δ). The NMR spectrum of Sm complex (figure 1) displays a sharp singlet at 3.02 ppm (δ) for H_{66} of tptz, while a strong singlet at 6.97 ppm (δ) is assigned to the methine proton of tfaa. The large upfield shift of the H_{66} protons (−5.98 ppm (δ)) observed for the Sm complex has never been noted for any complex of Sm. We too have studied NMR of many samarium complexes but could never find such a large shift [16b, 28–30]. In fact, Sm is known to induce very small upfield shifts with good spin–spin splitting. Another feature of the NMR spectrum of this complex is that signals of tptz are not uniformly displaced. The H_{33} protons being closer to Sm are expected to be shifted more than the H_{44} protons. However, the H_{44} proton signal is much more displaced to higher fields than the H_{33} protons. Owing to short electron relaxation time (due to the uniquely low-energy first excited state of Eu^{3+}), the europium complexes are expected to give signals with fine structures. The line width of the resonances due to coordinated tptz for the europium complex is much narrower (figure 2), in fact comparable with the line width of the diamagnetic analogue. The H_{66} proton signal of tptz moves to 22.50 ppm (δ)

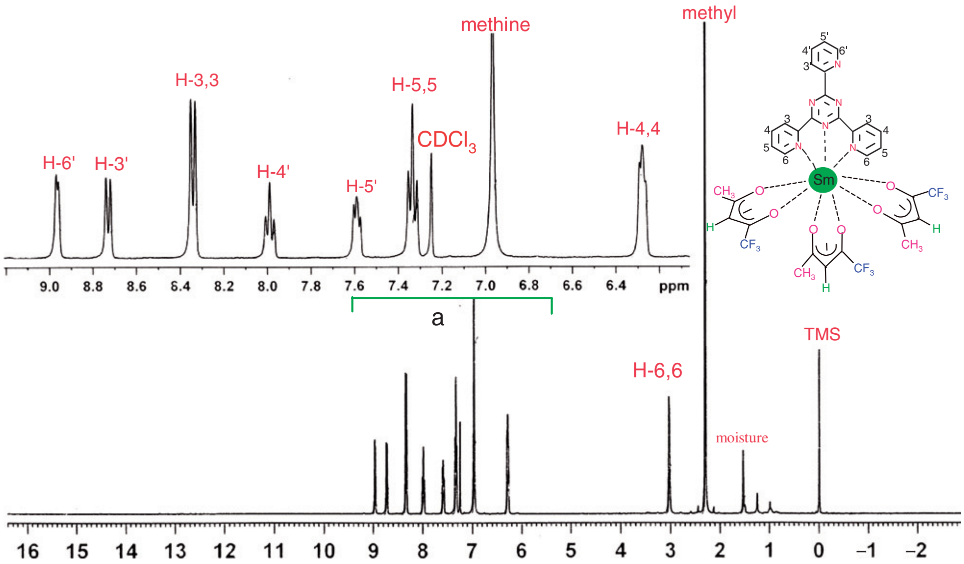

Figure 1. 400 MHz ^1H NMR spectrum of $[Sm(tfaa)_3(tptz)]$ in $CDCl_3$. Inset (a) higher resolution of the region 6.0–9.5 ppm (δ).

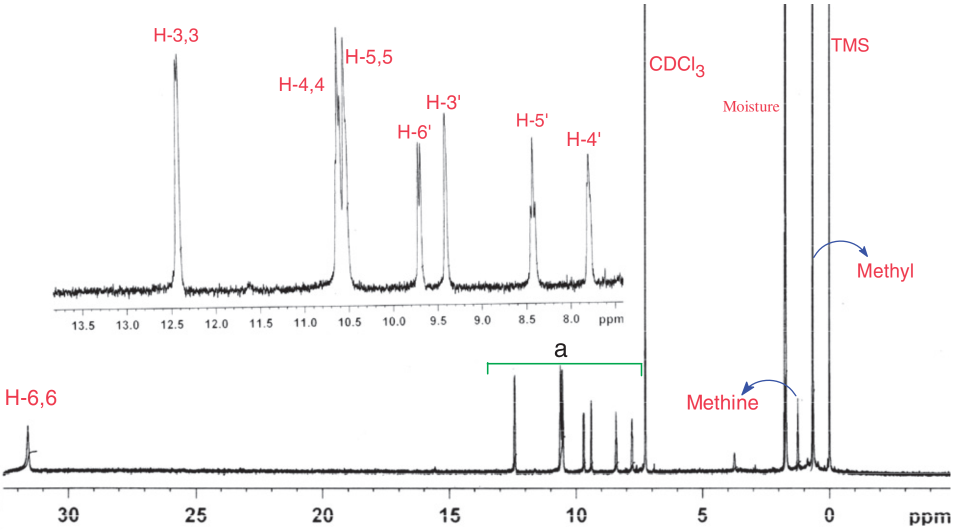

Figure 2. 400 MHz ^{1}H NMR spectrum of [Eu(tfaa)$_3$(tptz)] in CDCl$_3$. Inset (a) higher resolution of the region 7.5–13.5 ppm (δ). For protons numbering, see figure 1.

downfield as compared to its position in La analogue and appears at 31.50 ppm (δ) on the downfield side of TMS while the methyl resonance of tfaa moiety shifts to -1.19 ppm (δ) upfield as compared to the diamagnetic analogue. We compared the chemical shifts obtained for [Eu(tfaa)$_3$tptz] with those reported for [Eu(dbm)$_3$tptz] [24a] (where dbm is anion of dibenzoylmethane). The chemical shifts observed for the present complex are larger than for the dbm analogue. The larger chemical shifts could be related to (i) the asymmetry of tfaa resulting in greater anisotropy in "g" and (ii) the presence of highly electronegative fluorines which increase the residual acidity of the europium making it a better complexing site for incoming tptz. This would lead to greater covalency in bonding and would result in some change in the extent of overlap and, therefore, in the degree of covalency of the Ln–N (tptz) bonds.

An interesting feature of the spectra of the paramagnetic complexes is the position of the methine and methyl protons. Neodymium and samarium shift the resonances of the coordinated tptz to higher fields as compared to their positions in the diamagnetic complex; however, the tfaa protons (methyl and methine) move downfield. Similarly, for the europium complex the aromatic protons are shifted downfield compared to their position in the lanthanum complex, while the tfaa resonances move to highfield. The opposite shift direction of the β-diketone protons of these complexes reflects the importance of the geometric factor $3\cos^2\theta - 1$, in changing the sign of the paramagnetic shift. Therefore, it seems likely that the average geometric factor of the tptz and tfaa protons have opposite sign and the paramagnetic shift is exclusively due to dipolar interaction. This gains support from our earlier observations [15, 16b, 28, 30, 31] and the observation noted for Ln(C$_5$H$_5$)$_3$B (where B is an uncharged aprotic Lewis base), where the signal positions of B have sign opposite to that of the ring protons [32].

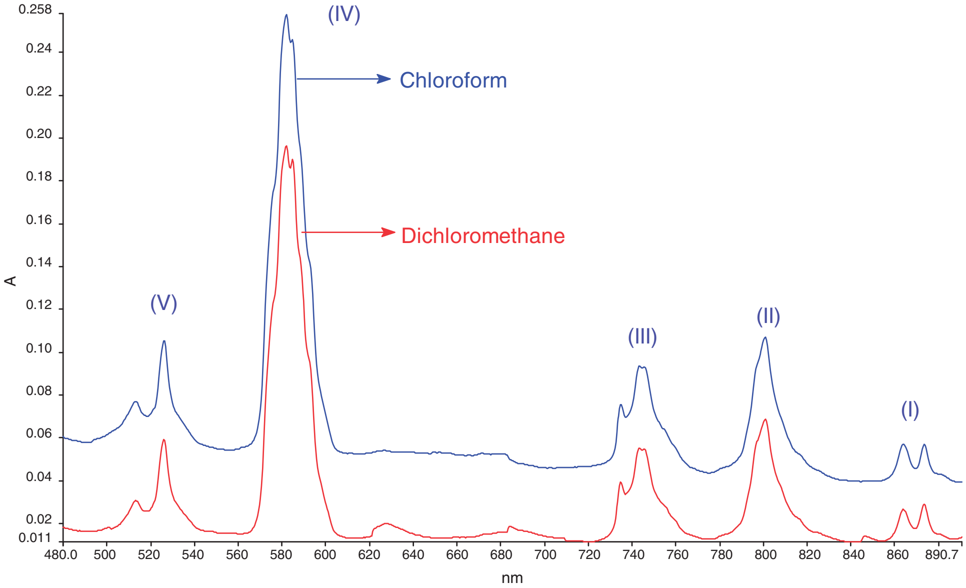

Figure 3. 4f–4f absorption spectra of [Nd(tfaa)$_3$tptz] in chloroform and dichloromethane; (I) $^4F_{3/2} \leftarrow {}^4I_{9/2}$, (II) $^2H_{9/2}$, $^4F_{5/2} \leftarrow {}^4I_{9/2}$, (III) $^4S_{3/2}$, $^4F_{7/2} \leftarrow {}^4I_{9/2}$, (IV) $^4G_{5/2}$, $^2G_{7/2} \leftarrow {}^4I_{9/2}$, and (V) $^2K_{13/2}$, $^4G_{7/2}$, $^4G_{9/2} \leftarrow {}^4I_{9/2}$ transitions.

3.3. *The 4f–4f absorption properties of [Nd(tfaa)$_3$tptz]*

The intensity of the absorption band can be expressed in terms of oscillator strength ($P \times 10^{-6}$). Experimentally, it is related to the integrated area of the absorption band and can be expressed in terms of absorption coefficient $\varepsilon(\nu)$ and the energy of the transition "ν" (cm^{-1}) as [33]

$$P = 4.31 \times 10^{-9}\left[\frac{9\eta}{(\eta^2+2)^2}\right]\int \varepsilon(\nu)\mathrm{d}\nu \tag{1}$$

where η is the refractive index of the solution and $\varepsilon(\nu)$ is the molar extinction coefficient at wavelength ν. The oscillator strength of the transitions is determined by evaluating the area under the peak.

Absorption spectra of the complex were recorded in a series of non-aqueous solvents (chloroform, dichloromethane, acetonitrile, ethanol, nitromethane, nitrobenzene, pyridine, and DMSO). The spectra are dominated by spin allowed π–π^* transitions of β-diketone (tfaa) and tptz in the ultraviolet region (200–400 nm). Tfaa and tptz show strong absorptions at 255 and 290 nm, respectively. The spectrum of the tptz complex contains essentially the combined ligand absorption at $\lambda_{\max} = 295$ nm. This band is shifted to longer wavelength (red shift) due to coordination of the ligand to neodymium (figure S6). In the visible region, the spectrum of the complex shows typical parity-forbidden narrow 4f–4f absorptions originating from the $^4I_{9/2}$ ground state to the various excited states of Nd(III) (figure 3). The transitions observed are $^4F_{3/2} \leftarrow {}^4I_{9/2}$ (Nd-I, 1.26×10^{-6}); $^2H_{9/2}$, $^4F_{5/2} \leftarrow {}^4I_{9/2}$ (Nd-II, 7.84×10^{-6}); $^4S_{3/2}$, $^4F_{7/2} \leftarrow {}^4I_{9/2}$ (Nd-III, 7.90×10^{-6}); $^4G_{5/2}$, $^2G_{7/2} \leftarrow {}^4I_{9/2}$ (Nd-IV, 8.60×10^{-6}); and $^2K_{13/2}$, $^4G_{7/2}$, $^4G_{9/2} \leftarrow {}^4I_{9/2}$

Table 2. Oscillator strength of $[Nd(tfaa)_3(tptz)]$ in non-aqueous solvents.

			Oscillator strength $P \times 10^{-6}$ solvents							
Transitions	Spectral ranges (cm^{-1})[a]	Nd^{3+} aqua ion ($P \times 10^{-6}$)	A	B	C	D	E	F	G	H
Nd^{3+} transitions ($\leftarrow {}^4I_{9/2}$)										
${}^4F_{3/2}$	10,784–11,761	1.26	2.60	2.54	1.66	1.57	1.82	2.64	2.12	2.31
${}^4F_{5/2}$, ${}^2H_{9/2}$	11,910–12,880	7.84	8.69	7.88	6.19	6.39	6.91	8.76	7.56	8.35
${}^4F_{7/2}$, ${}^4S_{3/2}$	12,911–13,890	7.90	8.49	7.98	5.83	6.12	6.58	8.42	7.48	8.13
${}^4G_{5/2}$, ${}^2G_{7/2}$	16,389–17,770	8.60	56.05	52.94	41.96	41.66	46.02	59.42	51.72	56.75
${}^4G_{7/2}$, ${}^4G_{9/2}$, ${}^2K_{13/2}$	18,169–20,098	6.20	11.89	10.35	8.27	8.39	10.00	10.06	11.26	12.35

A = chloroform; B = dichloromethane; C = DMSO; D = ethanol; E = acetonitrile; F = pyridine; G = nitrobenzene; H = nitromethane.

[a] Spectral ranges observed for the transition vary from solvent to solvent, so the values listed here are only meant to indicate the approximate location.

(Nd-V, 6.20×10^{-6}). The values in parentheses are the oscillator strength of the Nd^{3+} aqua ion. The oscillator strength of the transition of the complex, determined from the spectra using equation (1), is given in table 2. Among these transitions, the most intense is Nd-IV followed by Nd-V. The transition ${}^4G_{5/2}$, ${}^2G_{7/2} \leftarrow {}^4I_{9/2}$ located near the middle of the visible region (16,389–17,770 cm^{-1}) has very peculiar features with regard to its relative intensity and unusual sensitivity to the ligand environment around neodymium. It has large $U^{(2)}$ and $U^{(4)}$ matrix elements [33]. The relatively high intensity and unusual sensitivity to chemical environment about the neodymium ion have led to its classification as *hypersensitive* [34, 35]. Its behavior is in sharp contrast to many other typically weak and consistently unvaried, normal f–f transitions [35]. The oscillator strength of this transition increases 5–7-fold on going from the Nd^{3+} aqua-ion to the complex in any of the solvents used. The largest intensification is noted in pyridine which is followed by non-coordinating solvents chloroform and dichloromethane in table 2. Pyridine is especially effective in promoting 4f–4f electric dipole intensity in lanthanide complexes [36–40]. It is reasonable to associate this increase with ligand polarization effects such as those proposed by Mason, Peacock, and Stewart in their theory of hypersensitivity [41, 42]. The oscillator strengths are relatively low in coordinating solvents, except pyridine, lower than the value in non-coordinating chloroform. These lower values reflect influence of the solvents on the field around the Nd^{3+} ion and these solvents transform the field more symmetric. We compare the oscillator strength of the hypersensitive transition of the present complex with that observed for the analogous nine-coordinate hexafluoroacetylacetone (hfaa) complex, $[Nd(hfaa)_3tptz]$ (49×10^{-6}) [43], in chloroform, and note that the value is higher for the complex under study. The higher value could be related to the unsymmetrical structure of tfaa as compared to hfaa, which generates a more asymmetric field around the Nd^{3+} ion. It suggests the premise that the oscillator strength of the hypersensitive transition depends on the asymmetry of the field around the lanthanide ion.

3.3.1. Band shape. Both band shape and intensity of the hypersensitive transition have been used as qualitative indication of symmetry and coordination number [13–15]. The band shapes of the hypersensitive transition of the complex in different solvents are

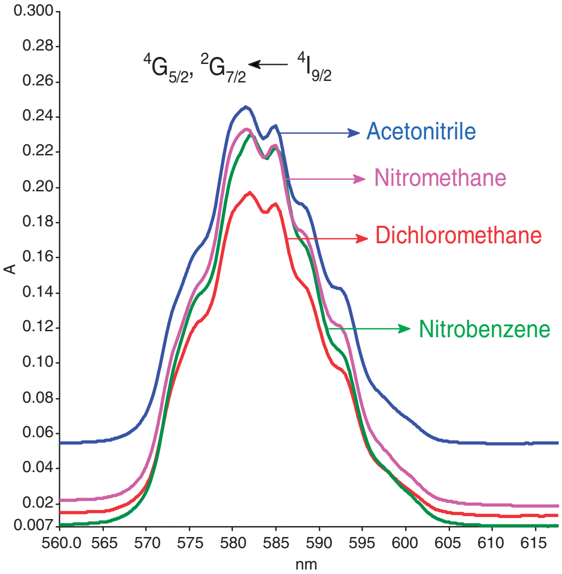

Figure 4. $^4G_{5/2}$, $^2G_{7/2} \leftarrow {}^4I_{9/2}$ (Nd-IV) transition of [Nd(tfaa)$_3$tptz] in acetonitrile, nitromethane, dichloromethane, and nitrobenzene.

shown in figures 3–5. Chloroform and dichloromethane are non-coordinating solvents and the band shape in these solvents is used as standard (i.e., band shape of the transition of the complex arising in non-coordinating solvents) for comparison with the band shape in the other solvents. The band shape of the hypersensitive transition of the complex in both the solvents is similar. The ligand field splitting, which is unsymmetrical in both solvents, is more prominent in dichloromethane. The band shapes of acetonitrile, nitromethane, and nitrobenzene resemble the band shape in dichloromethane (figure 4), while the band shapes in ethanol and pyridine are similar to that in chloroform (figure 5). Therefore, it is concluded that these solvents (with the exception of DMSO) do not coordinate with neodymium, and the different magnitude of the oscillator strength is due to the different nature of the solvents which generates the varying magnitude of the field. Those which bring more symmetry of the field around neodymium are responsible for the lower value of the oscillator strength, and those solvents which make the field more asymmetric lead to increase in oscillator strength. The band shape of the hypersensitive transition $^4G_{5/2}$, $^2G_{7/2} \leftarrow {}^4I_{9/2}$ of the present complex is distinctly different from those reported for typical eight- and ten-coordinate neodymium β-diketonate complexes [15–18, 44]. However, the band shape is similar to the nine-coordinate [Nd(hfaa)$_3$tptz] [43]. The ligand-field splitting in the hypersensitive band is unsymmetrical compared to the hfaa complex since tfaa is an unsymmetrical ligand.

We have also investigated the 4f–4f absorption spectrum of [Nd(tfaa)$_3$(H$_2$O)] in chloroform. Absorption spectra are given in figure S7 and the oscillator strengths are tabulated in table S1. Both [Nd(tfaa)$_3$tptz] and [Nd(tfaa)$_3$(H$_2$O)] are in unsymmetrical coordination environments. The band shape of [Nd(tfaa)$_3$(H$_2$O)] in chloroform is similar to the band shape of seven-coordinate [Nd(fod)$_3$(μ-pyz)Nd(fod)$_3$]. The oscillator strength of the hypersensitive transition of [Nd(tfaa)$_3$(H$_2$O)] in chloroform

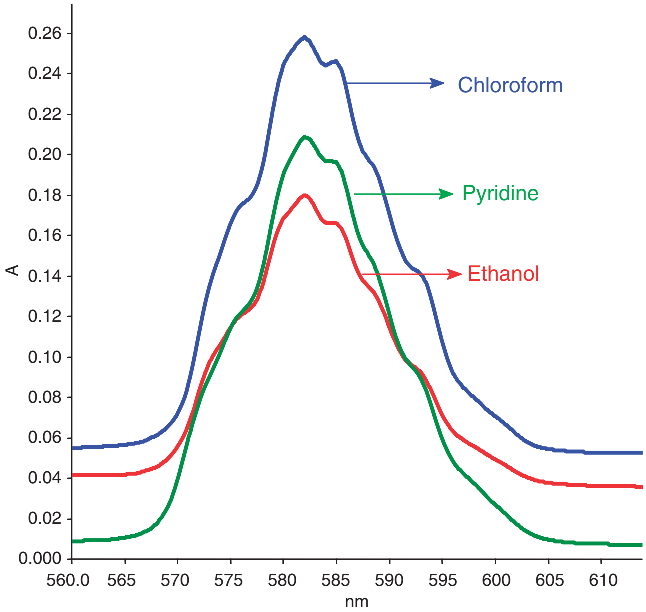

Figure 5. $^4G_{5/2}$, $^2G_{7/2} \leftarrow {}^4I_{9/2}$ (Nd-IV) transition of [Nd(tfaa)$_3$tptz] in chloroform, pyridine, and ethanol.

(49.13×10^{-6}) is lower than that for the tptz complex. The higher value of the oscillator strength lies in the larger number of Nd–N bonds in the tptz complex which leads to greater covalency in its bonding, suggesting the premise that the hypersensitivity depends on the covalency [35]. The band shapes of the tptz complex and the chelate are distinctively different, indicating that neodymium has different environments in the two complexes.

3.3.2. Absorption properties in DMSO. The hypersensitive transition is particularly sensitive to changes in coordination structure around neodymium and yields important information on the symmetry of the species in solution. The oscillator strength increases with increasing asymmetry of the field around the lanthanide [45, 46], while an increase in the symmetry of the field lowers the oscillator strength. The oscillator strength of the hypersensitive transition (Nd-IV) of the complex in DMSO is 42×10^{-6}, which is lower than the value in chloroform and dichloromethane. It indicates that the symmetry of the field around neodymium in DMSO has changed and becomes less asymmetric compared to the field in chloroform/dichloromethane. The band shape of the Nd-IV transition is distinctly different from the band shape (figure 6) arising in any of the other solvents used, also supporting that the symmetry has changed in this solvent. The band shape in DMSO resembles the band shape of this transition for typical eight-coordinate β-diketone neodymium complexes in non-coordinating solvents [15, 16a, 17, 18, 40] and seven-coordinate in coordinating solvents [30, 47]. This is only possible if the complex dissociates in this solvent and acquires an eight-coordinate structure (geometry). DMSO, which has a very high Gutmann donor number (29.8), could invade the coordination environment and may enter the inner coordination sphere of the

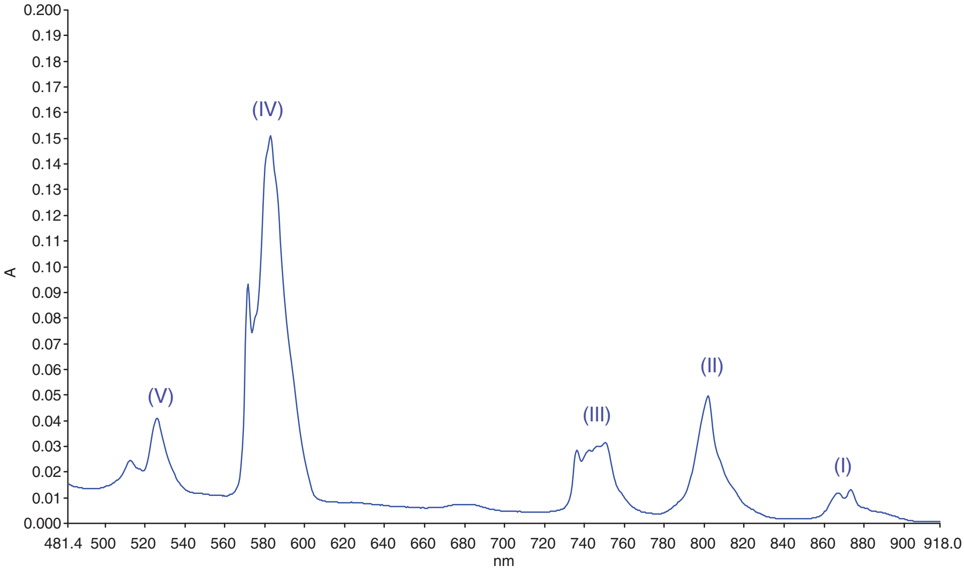

Figure 6. 4f–4f absorption spectrum of [Nd(tfaa)$_3$tptz] in DMSO; (I) $^4F_{3/2} \leftarrow {}^4I_{9/2}$, (II) $^2H_{9/2}$, $^4F_{5/2} \leftarrow {}^4I_{9/2}$, (III) $^4S_{3/2}$, $^4F_{7/2} \leftarrow {}^4I_{9/2}$, (IV) $^4G_{5/2}$, $^2G_{7/2} \leftarrow {}^4I_{9/2}$, and (V) $^2K_{13/2}$, $^4G_{7/2}$, $^4G_{9/2} \leftarrow {}^4I_{9/2}$ transitions.

neodymium by replacing tptz. The NMR spectrum of the neodymium complex in DMSO-d$_6$ shows four signals of equal intensity (two doublets and two triplets) due to free tptz in the range 7.72–8.91 ppm (δ), while no signal due to free tfaa is observed. The displacement of heterocyclic amines from many *tris*(β-diketonate)lanthanide(III) heterocyclic amine complexes and coordination of two DMSO molecules, in DMSO solution, have been reported from this laboratory [40, 44, 48]. Coordination of two DMSO molecules to [Ln(β-diket)$_3$] leading to the formation of [Ln(β-diket)$_3$(DMSO)$_2$] is available in the literature [44, 49]. Therefore, it is certain that two DMSO molecules have coordinated to neodymium by replacing tptz and making the Nd(III) eight-coordinate as shown below:

$$[\mathrm{Nd(tfaa)_3tptz}] + 2\mathrm{DMSO} \rightarrow [\mathrm{Nd(tfaa)_3(DMSO)_2}] + \mathrm{tptz}$$

Thus, the complex which has nine-coordinate geometry in solid state and/or in chloroform solution acquires an eight-coordinate structure in DMSO. Similar results have been obtained for closely related Pr, Ho, and Er complexes [19, 20]. The number of coordinated DMSO further gets support from a recent report on the crystal structure of a closely related compound containing three β-diketone-like ligands and two DMSO molecules [50].

3.4. *Photoluminescence*

Room temperature excitation and emission spectra of the europium and samarium complexes were recorded in chloroform. The luminescence spectra of the europium complexes (figure 7) consist of several bands related to de-excitation from the lowest

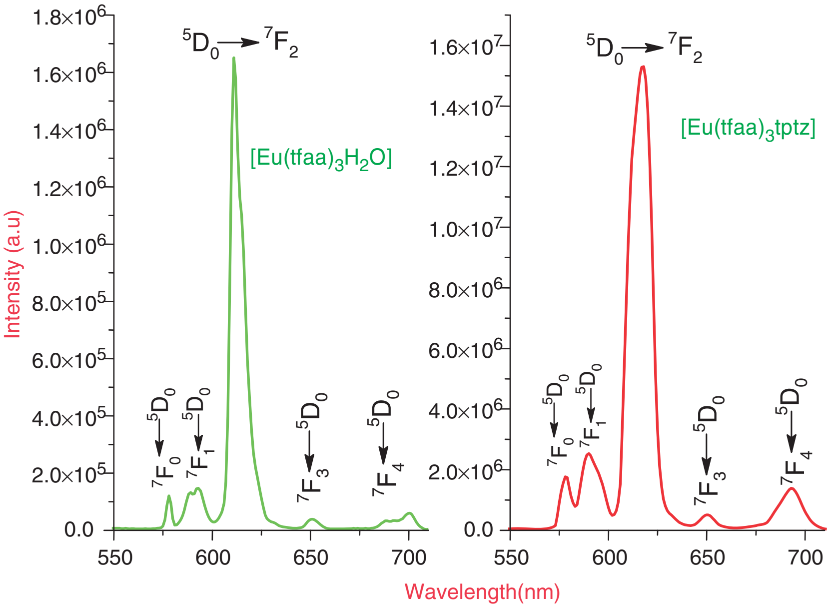

Figure 7. Emission spectra of [Eu(tfaa)$_3$H$_2$O] and [Eu(tfaa)$_3$(tptz)] in chloroform.

excited state, $^5D_0$, of the Eu^{3+}. The very intense band at 618 nm is due to $^5D_0 \rightarrow {}^7F_2$ transition. The four weak bands correspond to transitions from the $^5D_0$ state to the $^7F_0$, $^7F_1$, $^7F_3$, and $^7F_4$ levels, respectively. Recording the intensity of the $^5D_0 \rightarrow {}^7F_2$ transition as a function of excitation wavelength shows which transitions lead to population of the Eu^{+3} emitting state. The resulting excitation spectra display only one broad band at 365 for [Eu(tfaa)$_3$(tptz)] and 355 nm for [Eu(tfaa)$_3$H$_2$O], which are assigned to $S_0 \rightarrow S_1$ (figures S8 and S9) transition with the chromophores. It has been established that some transitions of the Eu(III) emission show energy or intensity variations which depend on the number, type, or arrangement of ligating atoms in the first coordination sphere of the metal [51]. The hypersensitive $^5D_0 \rightarrow {}^7F_2$ electric–dipole transition of [Eu(tfaa)$_3$(tptz)] and [Eu(tfaa)$_3$H$_2$O] is very intense due to ligand field effects and highly polarizable chemical environment around Eu(III) and is responsible for the brilliant red emission from these complexes. The intensity ratio of the hypersensitive $^5D_0 \rightarrow {}^7F_2$ transitions and the magnetic dipole $^5D_0 \rightarrow {}^7F_1$ transitions is about 6.03 for [Eu(tfaa)$_3$(tptz)] and 11.20 for [Eu(tfaa)$_3$H$_2$O], indicating that these complexes have structures with no imposed symmetry. Complexes with a centrosymmetric coordination sphere have $^5D_0 \rightarrow {}^7F_2/{}^5D_0 \rightarrow {}^7F_1$ intensity ratios lower than 0.7, whereas an intensity ratio higher than 8 is indicative of a low-symmetry environment around Eu(III) [52]. Only one line is observed for this non-degenerate $^5D_0 \rightarrow {}^7F_0$ emission transition of [Eu(tfaa)$_3$(tptz)] and [Eu(tfaa)$_3$H$_2$O], suggesting that only one type of Eu(III) species is present in solution.

The room temperature excitation spectra of [Sm(tfaa)$_3$(tptz)] and [Sm(tfaa)$_3$H$_2$O] were obtained by monitoring the 647 nm line of the $^4G_{5/2} \rightarrow {}^6H_{9/2}$ emission. It contains a broad band that corresponds to the excitation of the organic chromophores ($S_0 \rightarrow S_1$) and several weak peaks corresponding to intraconfigurational f–f transitions from the

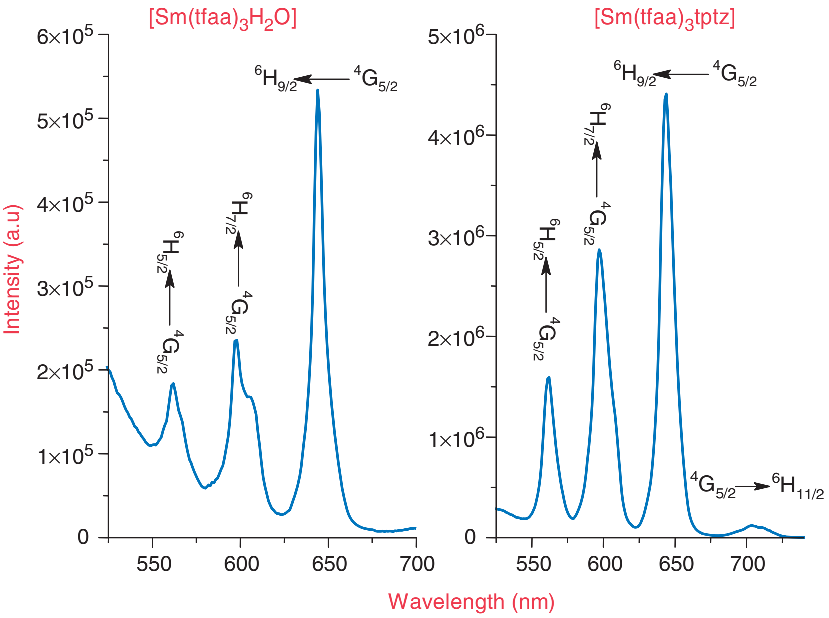

Figure 8. Emission spectra of [Sm(tfaa)$_3$H$_2$O] and [Sm(tfaa)$_3$(tptz)] in chloroform.

ground-state of Sm(III) (figures S10 and S11). The emission transitions observed for [Sm(tfaa)$_3$(tptz)] and [Sm(tfaa)$_3$H$_2$O] appear between 550 and 750 nm (figure 8). The emission transitions observed are $^4G_{5/2} \rightarrow {}^6H_{5/2}$ (forbidden transition), $^4G_{5/2} \rightarrow {}^6H_{7/2}$ (magnetic transition), and $^4G_{5/2} \rightarrow {}^6H_{9/2}$ (electric–dipole transition). Of the three transitions, the electric–dipole $^4G_{5/2} \rightarrow {}^6H_{9/2}$ hypersensitive transition is most intense and is responsible for the pink luminescence [16b, 18]. The $^4G_{5/2} \rightarrow {}^6H_{7/2}$ (607 nm) emission transition of [Sm(tfaa)$_3$(tptz)] has no Stark component, while this transition in the case of [Sm(tfaa)$_3$H$_2$O] has a Stark component, reflecting a higher local symmetry around Sm(III) in [Sm(tfaa)$_3$(tptz)] as compared to [Sm(tfaa)$_3$H$_2$O].

The luminescences from Sm(III) and Eu(III) tptz complexes are more intense than their respective chelates. Therefore, it is concluded that tptz is a synergic agent, which not only saturates the coordination sphere but also precludes the possibility of coordination of water/solvent molecules which may quench the luminescence.

4. Conclusion

We have synthesized nine-coordinate lanthanide complexes in which the lanthanide ions are coordinated to three N-atoms of 2-pyridyl units besides six oxygen atoms of tfaa units. The enhanced emission of tptz complexes over their respective chelates could be due to efficient energy transfer from the triplet-state of the ligands to the Eu(III) and Sm(III) emissive levels. The tptz provides additional advantage of site protection. The hypersensitive transition $^5D_0 \rightarrow {}^7F_2$ of the Eu(III) complex is very strong, which reflects the polarizable chemical environment around Eu(III) and is responsible for the *brilliant* *red* emission from this complex. The intensity ratio of the hypersensitive $^5D_0 \rightarrow {}^7F_2$ transition and the magnetic dipole $^5D_0 \rightarrow {}^7F_1$ transition is about 6.03 for the tptz complex and 11.20 for the chelate, which indicates that these complexes have structures with no imposed symmetry. The NMR signals of the tptz and diketone protons are shifted in opposite directions for paramagnetic complexes. The paramagnetic shift is dipolar in nature. The DMSO replaces tptz from the inner-coordination sphere with two DMSO molecules coordinating in an eight-coordinate structure, $[Nd(tfaa)_3(DMSO)_2]$, in this solvent. The band shape of the $^4G_{5/2}$, $^2G_{7/2} \leftarrow {}^4I_{9/2}$ hypersensitive transition of the tptz complex and the chelate are similar to those reported for typical nine- and seven-coordinate neodymium complexes of β-diketonates, respectively.

Acknowledgments

Part of the work was supported by the UGC Special Assistance Programme of the Department of Chemistry, Jamia Millia Islamia (No. F.540/17/DRS/2007/SAP-1). R. Ilmi thanks the University Grants Commission for the award of a BSR fellowship.

References

[1] E.G. Moore, A.P.S. Samuel, K.N. Raymond. *Acc. Chem. Res.*, **42**, 542 (2009).
[2] J. Kido, Y. Okamoto. *Chem. Rev.*, **102**, 2357 (2002).
[3] J.-C.G. Bunzli. In *Lanthanide Probes in Life, Chemical and Earth Sciences: Theory and Practice*, J.-C.G. Bunzli, G.R. Choppin (Eds), Chap. 7. Elsevier Science Publ. B.V., Amsterdam (1989).
[4] G. Blasse, B.C. Grabmaier. *Luminescent Materials*, Springer, New York (1994).
[5] T.R. Krishna, M. Parent, M.H.V. Werts, L. Moreaux, S. Gmouh, S. Charpack, A.-M. Caminade, J.-P. Majoral, D.M. Blanchar. *Angew. Chem., Int. Ed.*, **45**, 4645 (2006).
[6] S.V. Eliseeva, J.-C.G. Bünzli. *Chem. Soc. Rev.*, **39**, 189 (2010).
[7] K. Binnemans. In *Handbook on the Physics and Chemistry of Rare Earths*, K.A. Gschneidner Jr, J.-C.G. Bünzli, V.K. Pecharsky (Eds), Vol. 35, Chap. 225. Elsevier, Amsterdam (2005).
[8] R.E. Sievers, J.E. Sadlowski. *Science*, **201**, 217 (1978).
[9] P. Gawryszewska, J. Sokolnicki, J. Legendziewicz. *Coord. Chem. Rev.*, **249**, 2489 (2005).
[10] L. Yang, Z. Gong, D. Nie, B. Lou, Z. Bian, M. Guan, C. Huang, H.J. Leeb, W.P. Baik. *New J. Chem.*, **30**, 791 (2006).
[11] J.-M. Lehn. *Angew. Chem., Int. Ed. Engl.*, **29**, 1304 (1990).
[12] L.R. Melby, N.J. Rose, E. Abramson, J.C. Caris. *J. Am. Chem. Soc.*, **86**, 5117 (1964).
[13] K. Iftikhar, M. Sayeed, N. Ahmad. *Inorg. Chem.*, **21**, 80 (1982).
[14] A. Bellusci, G. Barberio, A. Crispini, M. Ghedini, M. La Deda, D. Pucci. *Inorg. Chem.*, **44**, 1818 (2005).
[15] Z. Ahmed, K. Iftikhar. *Inorg. Chim. Acta*, **363**, 2606 (2010).
[16] (a) M. Irfanullah, K. Iftikhar. *Inorg. Chem. Commun.*, **12**, 296 (2009); (b) M. Irfanullah, K. Iftikhar. *J. Photochem. Photobiol. A*, **224**, 91 (2011).
[17] M. Irfanullah, K. Iftikhar. *Inorg. Chem. Commun.*, **13**, 694 (2010).
[18] R. Ilmi, K. Iftikhar. *Inorg. Chem. Commun.*, **13**, 1552 (2010).
[19] M. Irfanullah, K. Iftikhar. *J. Fluoresc.*, **21**, 81 (2011) 21, 673 (2011).
[20] M. Irfanullah, K. Iftikhar. *J. Lumin.*, **130**, 1983 (2010).
[21] G. Ionova, C. Rabbe, R. Guillaumont, S. Ionov, C. Madic, J.-C. Krupa. *New J. Chem.*, **26**, 234 (2002).
[22] M.G.B. Drew, M.J. Hudson, P.B. Iverson, C. Madic. *Acta Crystallogr.*, **C56**, 434 (2000).
[23] G.Y.S. Chan, M.G.B. Drew, M.J. Hudson, N.S. Isaacs, P. Byers. *Polyhedron*, **15**, 3385 (1996).
[24] (a) C.R. De Silva, J. Wang, M.D. Carducci, S.A. Rajapakshe, Z. Zheng. *Inorg. Chim. Acta*, **357**, 630 (2004); (b) C.R. De Silva, R. Wang, Z. Zheng. *Polyhedron*, **25**, 3449 (2006); (c) C.R. De Silva, J.R. Maeyer, A. Dawson, Z. Zheng. *Polyhedron*, **26**, 1229 (2007).
[25] M. Sayeed, N. Ahmed. *J. Inorg. Nucl. Chem.*, **43**, 3197 (1981).

[26] J.M. Curtis, P.J. Derrick, A. Schnell, E. Constantin, R.T. Gallagher, J.R. Chapman. *Inorg. Chim. Acta*, **201**, 197 (1992).
[27] Y.Q. Lu, Z.H. Deng. *Practical Infrared Spectrum Parse* [M], Electron Industry Press of China, Beijing (1989).
[28] K. Iftikhar. *Polyhedron*, **15**, 1113 (1996).
[29] A.A. Khan, K. Iftikhar. *Indian J. Chem.*, **39A**, 1286 (2000).
[30] M. Irfanullah, K. Iftikhar. *Inorg. Chem. Commun.*, **13**, 1234 (2010).
[31] Z. Ahmed, K. Iftikhar. *Inorg. Chim. Acta*, submitted.
[32] R.D. Fischer. In *NMR of Paramagnetic Molecule: Principles and Applications*, G.N. La Mar, W.D. Horrocks Jr, R.H. Holm (Eds), p. 521, Academic Press, New York (1973).
[33] W.T. Carnall, P.R. Fields, B.G. Wybourne. *J. Chem. Phys.*, **42**, 3797 (1965).
[34] A.A. Khan, H.A. Hussain, K. Iftikhar. *Spectrochim. Acta A*, **59**, 1051 (2003).
[35] D.E. Henrie, R.L. Fellows, G.R. Choppin. *Coord. Chem. Rev.*, **18**, 199 (1976).
[36] A.A. Khan, H.A. Hussain, K. Iftikhar. *Spectrochim. Acta A*, **59**, 1051 (2003).
[37] H.A. Hussain, K. Iftikhar. *Spectrochim. Acta A*, **59**, 1061 (2003).
[38] H.A. Hussain, A.A. Ansari, K. Iftikhar. *Spectrochim. Acta A*, **60**, 873 (2004).
[39] A.A. Khan, K. Iftikhar. *Polyhedron*, **16**, 4153 (1997).
[40] A.A. Ansari, M. Irfanullah, K. Iftikhar. *Spectrochim. Acta A*, **67**, 1178 (2007).
[41] S.F. Mason, R.D. Peacock, B. Stewart. *Mol. Phys.*, **30**, 1829 (1975).
[42] R.D. Peacock. *Mol. Phys.*, **33**, 1239 (1977).
[43] Z. Ahmed, K. Iftikhar. *Inorg. Chem. Commun.*, **13**, 1253 (2010).
[44] A.A. Ansari, R. Ilmi, K. Iftikhar. *J. Lumin.*, **132**, 51 (2012).
[45] C.K. Jorgensen, B.R. Judd. *Mol. Phys.*, **8**, 281 (1964).
[46] B.R. Judd. *J. Chem. Phys.*, **44**, 839 (1966).
[47] K. Iftikhar. *Inorg. Chim. Acta*, **128**, 273 (1987).
[48] K. Iftikhar, unpublished results.
[49] H.F. Brito, O.L. Malta, J.F.S. Menezes. *J. Alloys Compd.*, **303–304**, 336 (2000).
[50] M. Correa-Ascencio, E.K. Galván-Miranda, F. Rascón-Cruz, O. Jiménez-Sandoval, S.J. Jiménez-Sandoval, R. Cea-Olivares, V. Jancik, R.A. Toscano, V. García-Montalvo. *Inorg. Chem.*, **49**, 4109 (2010).
[51] F.S. Richardson. *Chem. Rev.*, **82**, 541 (1982).
[52] (a) A.F. Kirby, D. Foster, F.S. Richardson. *Chem. Phys. Lett.*, **95**, 507 (1983); (b) A.F. Kirby, F.S. Richardson. *J. Phys. Chem.*, **87**, 2544 (1983).